Comparison of computed tomographic and pathologic findings in 17 dogs with primary adrenal neoplasia

Tommaso Gregori, Panagiotis Mantis, Livia Benigni, Simon L. Priestnall and Christopher R. Lamb

From the Department of Clinical Sciences and Services (Gregori, Mantis, Benigni, Lamb) and the Department of Pathology and Pathogen Biology (Priestnall), The Royal Veterinary College, University of London

Address correspondence to: Tommaso Gregori, Department of Clinical Sciences and Services, The Royal Veterinary College, North Mymms, Hertfordshire AL9 7TA, U.K.
Email: tgregori@rvc.ac.uk

Key words: adrenal gland, computed tomography, dog, neoplasia

Running head: CT and histology of adrenal neoplasia

Abstract:

The CT appearance of canine adrenal masses has been reported, but associations between imaging features and pathologic features of these lesions have not been investigated in detail. In order to test the associations between different types of adrenal neoplasia and their CT and pathologic features, a retrospective study was performed. Seventeen dogs that had histologic diagnosis of primary adrenal neoplasia following a CT contrast of the abdomen and surgical resection of the mass or necropsy examination were included in the study. CT images and histopathologic specimens were reviewed independently by two radiologists and a pathologist, respectively. Diagnoses were adenocarcinoma in 9 (53%) dogs, pheochromocytoma in 5 (29%) dogs, and adenoma in 3 (18%) dogs. Pheochromocytoma was associated with CT signs of vascular invasion (likelihood ratio=4.8, 95% CI=1.3-18.3, *P*=0.03) and macroscopic vascular invasion (likelihood ratio=9.6, 95% CI=1.4-65.9, *P*=0.02). There was excellent agreement between signs of vascular invasion in CT images and vascular invasion at surgery or necropsy (kappa=0.86, *P*=0.001). A peripheral contrast-enhancing rim in delayed post-contrast CT images was associated with fibrous encapsulation of the tumor (kappa=0.53, P=0.05), and a heterogeneous pattern of contrast distribution in delayed post-contrast CT images was associated with adrenal hemorrhage or infarction on histological examination (kappa=0.45, *P*=0.05). Although CT enabled assessment of features that reflect their biological behavior of adrenal neoplasms with good agreement with pathological findings, the overlap in pathologic features between tumor types will limit the potential for those tumor types to be distinguished by CT.

Introduction:

Primary adrenal neoplasia is an uncommon, but well recognized condition in dogs[1]. Adrenal adenoma, adenocarcinoma and pheochromocytoma are considered the most common tumors affecting the canine adrenal gland[1,2,3,4]. Adrenal myelolipoma, a benign tumor composed of adipose tissue and hematopoietic cells, has also been reported in dogs[5,6]. Adrenal neoplasms may cause a range of clinical signs, depending primarily on their endocrinological activity. Adrenocortical neoplasms producing cortisol cause signs of canine Cushing's syndrome, including polyuria/polydipsia, polyphagia, hair loss, hepatomegaly and pendulous abdomen. Epinephrine or norepinephrine-secreting pheochromocytomas are associated with signs such as weakness, collapse, cardiac dysrhythmia or hypertension. Endocrinologically inactive adrenal neoplasms usually cause non-specific clinical signs, including weight loss. Adrenal gland masses, both neoplastic and hyperplastic, are recognized frequently during abdominal imaging in older dogs, and in many instances are thought to be clinically silent 'incidentalomas'[4].

Imaging of suspected adrenal neoplasia in dogs is performed with the intention of determining the anatomical origin of the tumor, its morphologic features, which may reflect biological behavior, and to look for signs of metastasis. Of the various adrenal neoplasms, malignant pheochromocytomas are considered the most aggressive, with direct invasion of adjacent vasculature reported in up to 85% dogs and distant metastasis in up to 40% dogs[1,7,8].

In humans computed tomography (CT) plays an important role in characterizing adrenal neoplasms[9,10]. The majority of adrenal adenomas and myelolipomas in humans contain a significant amount of intracellular fat, hence these benign tumors usually have lower x-ray attenuation than malignant adrenal neoplasms[9] and the combination of low density

values (<10 HU) in non-enhanced CT images and early contrast wash-in/wash-out through the mass seen in benign tumors, enables correct classification of benign versus malignant adrenal lesions in up to 96% of affected humans[11]. CT also enables detection of tumor- or blood clot-thrombus in vessels adjacent to the adrenal glands, which occurs as a result of invasion by malignant neoplasms[12].

CT has also been found to be a useful method for imaging the adrenal glands in dogs. The CT appearance of adrenal glands has been described in healthy dogs[13,14], dogs with pituitary-dependent hyperadrenocorticism[15,16,17], and dogs with primary adrenal neoplasia[5,18,19,20]. As in humans, CT is an accurate method for detection of vascular invasion by malignant adrenal neoplasms, with 92% sensitivity and 100% specificity in one study[19]. The histologic composition of adrenal neoplasms is somewhat heterogeneous in both humans and dogs with variable amounts of hemorrhage, necrosis and/or mineralization occurring in benign and malignant neoplasms[10, 21, 22]. As a result, different tumor types may appear similar in CT images[5,19]; however, previous studies of the CT appearance of canine adrenal tumors have not investigated in detail their imaging-pathologic correlations.

The aims of the present study were to: (1) test the associations between different types of adrenal neoplasia and histopathologic and CT imaging features (2) assess the agreement between CT imaging findings and analogous histopathologic features of adrenal neoplasms.

Methods:

Patient selection- The electronic patient record system at the Queen Mother Hospital for Animals (QMHA) was searched using the terms *adrenalectomy, adrenal mass,*

computed tomography, and *dog*. Pathological data for patients retrieved by this search was then sought in the QMHA's clinical pathology database. Dogs that had abdominal CT, surgical resection of an adrenal mass or necropsy, and histological diagnosis of adrenal neoplasia were included in this study. The breed, age and gender of these dogs were recorded.

CT imaging- All CT exams were performed using the same 16-slice scanner (Mx8000 IDT, Philips, Best, The Netherlands) with dogs in sternal recumbency under general anesthesia or sedation. All CT studies included one pre-contrast acquisition and at least one post-contrast acquisition of the abdomen. Non-ionic iodinated contrast medium, Iohexol (Omnipaque 350 mg/mL, Nycomed, Oslo) was administered as a bolus injection at a dose of 2 mL/kg using, when available, a pressure injector (Stellant, Medrad, Indianola, PA.) at a rate of 2 mL/s. Post contrast scans were obtained at 30s (early phase) or at 120s (delayed phase) after the start of contrast injection. When contrast was administered by hand injection, a first scan was typically acquired within 60s of the start of injection, followed by another scan at 120s. CT machine settings for image acquisition varied depending on the size of the patient. Typical settings were: helical mode, 2-3 mm slice thickness, 1 s rotation time, 1.25 pitch, 90 or 120 kVp, 100-150 mA, 500 mm acquisition field of view, standard reconstruction algorithm and 512x512 matrix.

Two board-certified radiologists (LB, PM) unaware of the surgical and pathological results reviewed the images from the CT studies together and reached a consensus. CT images were displayed in an abdominal window (window level= 40 HU, window width= 400 HU) on a workstation using commercially available DICOM image viewing software (OsiriX 64-bit, version 5.2.2, Pixmeo, Switzerland). CT images were reviewed with respect to a set of pre-considered criteria as follows: maximum diameter (mm) of the

mass in any reformatted plane (transverse, sagittal or dorsal); adrenal mass outline (well demarcated VS irregularly demarcated); shape (rounded VS lobulated); pattern of pre-contrast attenuation (homogeneous VS heterogeneous); pattern of post-contrast enhancement (homogeneous VS heterogeneous) on early and delayed phases; presence of contrast enhancing peripheral rim on early and delayed phases; and irregular vessel lumen or intraluminal thrombus compatible with tumor invasion or blood clot within the ipsilateral phrenico-abdominal vein, renal vein or caudal vena cava. Average attenuation and standard deviation (SD) in Hounsfield Units (HU) of each adrenal mass was measured on pre-contrast, early- and delayed-phase post-contrast images by manually drawing a region of interest to fit the mass in each image in each plane in which the mass appeared largest. Attenuation data were regrouped into categories of contrast enhancement: slight (< 60HU), moderate (≥60, <110) and marked (≥110).

Pathology– The method of examining each adrenal mass (i.e. surgical adrenalectomy VS necropsy), laterality of the adrenal mass and the presence or absence of macroscopic vascular invasion were recorded. A board-certified pathologist (SP) reviewed archived histopathology samples from the adrenal lesions, being unaware of imaging findings. Variables evaluated based on review of ten x400 high power fields were: mitotic index, cellular differentiation (well-differentiated; moderately well-differentiated; poorly differentiated), percentage of necrosis (N0<10%; N1= 10%-25%; N2= 26%-50%; N3= >50%), presence of hemorrhage or infarction, presence of peripheral capsular invasion, microscopic vascularity (slight, moderate, marked) and presence of microscopic vascular invasion. Classification of tumor grade (high or low) was based on these results: tumor was considered of high grade if for 3 or more results were positive or classified in the higher category group. The pathologist formulated a final diagnosis (i.e. adrenocortical adenoma, adrenocortical adenocarcinoma or pheochromocytoma) for each adrenal mass.

Because low-grade adrenocortical adenocarcinomas and adenomas are often difficult to differentiate [7], the classification of benign VS malignant was based on combined criteria including mitotic index, tumor grade, capsular invasion and presence of microscopic vascular invasion.

Statistical analysis- Statistical calculations were performed using commercially available software (SPSS® Software, Version 20.0.0, IBM Corp, Armony, NY). Fisher's exact test was used to test the association between diagnosis (i.e. adrenocortical adenoma, adrenocortical adenocarcinoma or pheochromocytoma) and each of the following categorical variables: breed, gender, mitotic index, cellular differentiation, percentage of necrosis, presence of areas of hemorrhage or infarction, presence of peripheral capsular invasion, microscopic vascularity, presence of microscopic vascular invasion, macroscopic vascular invasion, tumor grade, outline, shape, pattern of pre-contrast attenuation, pattern of post-contrast enhancement on early and delayed phases, presence of contrast enhancing peripheral rim on early and delayed phases, presence of tumor invasion within the adjacent vasculature and degree of contrast enhancement on early and delayed phases. Monte Carlo estimation for Fisher's exact test was used when a count less than 5 elements per cell was expected in a variable including more than two categories. Likelihood ratios (and 95% confidence intervals, CI) were calculated for results with $P<0.05$. Continuous data (e.g. age, maximum diameter of the mass on CT, average HU on pre-contrast, early and delayed phases, difference of average HU between early or delayed post-contrast and pre-contrast phases) was tested for normality using the Shapiro-Wilk test, and relationships between these variables and diagnosis were tested using analysis of variance. For all statistical tests, results with $P<0.05$ were considered to be significant.

Certain CT features and pathological features were considered analogous. Agreement between the following binomial CT and histopathology features was tested using the kappa statistic: presence of areas of hemorrhage or infarction VS pattern of contrast enhancement on early and delayed phases, presence of peripheral capsular invasion VS mass outline, presence of peripheral capsular invasion VS contrast enhancing rim on early and delayed phase, presence of macroscopic vascular invasion VS presence of vascular invasion on CT post contrast images. Rank correlation between the following ordinal CT and histopathology features was tested using Kendall's Tau b or c tests: percentage of necrosis VS pattern of contrast enhancement on early and delayed phases, microscopic vascularity VS degree of contrast enhancement on early and delayed phase. Statistical tests were performed by two authors (TG, CRL).

Results:

Seventeen dogs with a total of 17 adrenal masses were included in this study. Tumors were diagnosed as adrenocortical adenocarcinoma (n=9, 53%), pheochromocytoma (n=5, 29%), and adrenocortical adenoma (n=3, 18%). These masses were analyzed either after they were removed by surgical adrenalectomy (n=15, 88%) or on post-mortem examination (n=2, 12%). More tumors affected the left adrenal gland (n=11, 65%) than the right (n=6, 35%). Median age of the patients was 10 years (range: 5-15 years). Breeds were German shepherd (n=2), Golden retriever (n=2) and Lurcher (n=2), Boxer (n=1), Cocker Spaniel (n=1), Collie (n=1), Fox Terrier (n=1), Jack Russell Terrier (n=1), Labrador (n=1), Miniature Poodle (n=1), Rottweiler (n=1), Shih Tzu (n=1), West Highland White terrier (n=1) and cross breed (n=1).

Relationships between tumor type and pathological findings are summarized in Table 1. The only significant association found was between pheochromocytoma and presence of macroscopic vascular invasion (likelihood ratio=9.6, 95% CI 1.4-65.9).

Relationships between tumor type and CT features are summarized in Table 2. In three dogs, only the early post-contrast CT images were available for review. There was a significant association between pheochromocytoma and CT signs of vascular invasion or thrombus formation (likelihood ratio=4.8, 95% CI 1.3-18.3). The higher mean HU pre-contrast for pheochromocytoma compared to other neoplasms was of borderline significance (P=0.06). No other significant associations were found.

Results of the agreement or correlation between analogous histopathological and CT findings are summarized in Table 3. There was moderate agreement between absence of peripheral capsular invasion by neoplastic cells on histopathology and the presence of an enhancing rim on post-contrast late phase CT images (kappa=0.53, *P*=0.05). There was excellent agreement with respect to presence of vascular invasion (kappa=0.86, *P*=0.001). In one dog the adrenal mass was considered to be invasive because of marked impingement on the caudal vena cava and focal irregularity in intraluminal contrast observed in CT images; however, no evidence of vascular invasion by this mass was identified during surgery or on histopathologic examination. There was moderate agreement between hemorrhage or infarction seen histologically and a heterogeneous pattern of post contrast enhancement in late phase CT images (kappa=0.45, *P*=0.05).

Discussion:

CT is now routinely used in referral practices for the preoperative assessment of dogs with an adrenal mass because it is considered more accurate than abdominal

ultrasonography for the detection of the vascular invasion[19]. In the present study there was excellent agreement between signs of vascular invasion in CT images and finding vascular invasion at surgery or necropsy. A discrepancy (false positive) was identified in only one dog; hence sensitivity, specificity and accuracy of CT for vascular invasion in this study were respectively 92%, 89% and 94%. The single erroneous CT interpretation of vascular invasion probably occurred because of the marked compression of the caudal vena cava by the adrenal mass, which caused narrowing of the vessel lumen. Such impingement may alter the blood flow and disrupt the pattern of post-contrast enhancement of these vessels, mimicking a thrombus, which is the principal imaging sign of vascular invasion. The presence of vascular invasion influences the choice of surgical approach for tumor resection[24], although there appear to be no significant differences in perioperative morbidity and mortality rates between patients with or without a tumor-associated thrombus.

Pheochromocytoma appears more likely to invade adjacent vessels than adrenocortical adenoma or adenocarcinoma (Fig. 1), as has been reported previously[25]; however, this finding at surgery or necropsy result was not associated with microscopic vascularity or histological signs of vascular invasion within this tumor. In two dogs, one with a high-grade pheochromocytoma and one with a high-grade adenocarcinoma, there was evidence of peripheral capsular invasion by the tumor, with additional focal infiltration of neoplastic cells in the adipose tissue surrounding the gland in the dog with pheochromocytoma. Pheochromocytoma invading the hypaxial and epaxial musculature has been reported in dogs[18,19], but this feature was not observed in dogs in the present study.

The presence of a peripheral contrast-enhancing rim in late phase CT images was associated with fibrous encapsulation of the tumor on histological examination (Fig. 2). A fibrous pseudocapsule (composed of compressed adjacent soft tissues), free of neoplastic cell infiltration is recognized more frequently in well-differentiated and low-grade tumors. All adrenal adenomas in the present study had both CT and histopathological features compatible with a pseudo-capsule around the tumor. Finding a peripheral contrast-enhancing rim and absence of signs of vascular invasion in CT images of an adrenal mass suggests benign behavior. In contrast, the capsular infiltration identified in two dogs with high-grade adenocarcinoma and pheochromocytoma, respectively, was indicative of the malignant biological behavior of these tumors.

Necrosis and hemorrhage are common in adrenal tumors[18,23], and these features were considered responsible for the variable echogenicity of adrenal tumors in one study[21]. Similarly, in the present study, the presence of hemorrhage or infarction within an adrenal mass was associated with a heterogeneous pattern of contrast enhancement on late phase CT images (Fig.3). Masses with a homogeneous post contrast enhancement were less likely to contain foci of hemorrhage or infarction. In a report of four dogs with pheochromocytoma, the adrenal masses also had variable appearance in CT images, with multiple foci of low attenuation interspersed with hyperattenuating, highly vascularized areas[18]. It may not be possible to distinguish types of adrenal tumor based on CT features such as pre-contrast pattern of attenuation or degree or pattern of post-contrast enhancement because hemorrhage or necrosis are liable to occur when any tumor reaches a certain size.

In humans, adrenal adenomas may be recognized by CT because of their characteristic low x-ray attenuation that occurs due to the presence of fat-laden cells in up to 70% of

these tumors[9,26]. Intracellular lipid-rich substances such as cholesterol and fatty acids have also been reported in canine patients with adrenal hyperplasia and adenomas[2]. A report of CT findings in a dog with bilateral adrenal adenomas and myelolipomas described one enlarged gland with a hypoattenuating center (-56HU) compatible with fat, while the contralateral adrenal gland was more homogeneous with a higher attenuation (39HU)[5]. The latter value is similar to the mean HU value (40.8HU) found for adenomas in pre-contrast CT images in the present study. These values are also similar to the HU values of 31.8 and 33.1 reported for hyperplastic adrenal glands in dogs with pituitary microadenoma or macroadenoma[15]. A recent study found that pheochromocytomas had higher mean attenuation (44.5HU) than adrenal adenocarcinomas (28.2HU)[27]. Interestingly, we also found evidence that the mean pre-contrast HU value for pheochromocytomas may be higher than for other adrenal neoplasms, although this result was of borderline significance.

Another criterion used in humans to differentiate adrenal adenomas from malignant tumors is the early contrast wash-out associated with adenomas that is observed in delayed (typically at 15 minutes) post-contrast images[11,28]. We found no significant differences in the degree of enhancement or HU values measured in post-contrast CT images of different tumor types. Similarly no significant differences were found in their microscopic vascularization. These results differ from results presented in two recent studies in which pheochromocytoma was found to have more marked contrast enhancement than adenocarcinoma[27,29]; however, it is uncertain if this difference in results occurred because of differences in the timing of post-contrast acquisitions as this information was not included.

The present study has several limitations. The relatively small number of adrenal tumors included limits the power of the statistical tests. Inclusion criteria (e.g. final histologic diagnosis after adrenalectomy or post mortem examination) may have caused a patient selection bias in favor of dogs with more marked clinical signs and more endocrinologically active or malignant tumors, such as some adenocarcinomas and malignant pheochromocytomas, at the expense of dogs with adenomas[7,25]. There are also limitations in the comparison of CT and pathological findings. Histologic sections reveal microscopic structures below the resolution of CT scanners, and usually cover only a small part of a lesion observed by CT, hence discrepancies in the presence and extent of reported abnormalities are inevitable. The retrospective nature of the study limited the amount of information available, particularly about other macroscopic pathologic features, which may have helped distinguish tumor types of strengthened imaging-pathological correlations.

Another possible limitation might be the method used to evaluate the microscopic vascularity of adrenal tumors, which was based on partially subjective criteria (pathologist's judgment, based on review of ten x400 high power fields for each slide). Quantitative methods of assessment of tumoral microvasculature (e.g. microscopic vascular density) have been reported as a method to evaluate the response of a tumor to antiangiogenic therapy.[30] It is unclear if this method offers advantages over the subjective method used because it is also susceptible to variability because of heterogeneity within a mass.

In conclusion, although CT enabled assessment of features that reflect the biological behavior of adrenal neoplasms with good agreement with pathological findings, the overlap in pathologic features between tumor types will limit the potential for those

299 tumor types to be distinguished by CT. Further studies of a larger number of dogs are
300 needed to support our results.

References:

1. Lunn KF, Page RL. Tumors of the endocrine system. In: Withrow SJ, Vail DM, Page RL (eds): Withrow & MacEwen's Small Animal Clinical Oncology. 5th ed. St.Louis, MO: Saunders Elsevier, 2013:504–531.

2. Capen CC. Tumors of the endocrine glands. In: Meuten DJ (ed): Tumors in Domestic Animals, 4th ed. Ames, IA: Blackwell Publishing, 2002;607–696.

3. Melian C, Perez-Alenza MD, Peterson ME. Hyperadrenocorticism in dogs. In: Ettinger SJ, Feldman EC (eds): Textbook of Veterinary Internal Medicine: Diseases of the Dog and Cat, 7th ed. St. Louis, MO: Saunders Elsevier, 2010;1816-1839.

4. Myers NC. Adrenal incidentalomas. Diagnostic workup of the incidentally discovered adrenal mass. Vet Clin North Am Small Anim Pract 1997;27:381-399.

5. Morandi F, Mays JL, Newman SJ, et al. Imaging diagnosis – bilateral adrenal adenomas and myelolipomas in a dog. Vet Radiol Ultrasound 2007;48:246–249.

6. Tursi M, Iussich S, Prunotto M, et al. Adrenal myelolipoma in a dog. Vet Pathol 2005; 42:232-235.

7. Barthez PY, Marks SL, Woo J, et al. Pheochromocytoma in dogs: 61 cases (1984–1995). J Vet Intern Med 1997;11:272-278.

8. Feldman EC, Nelson RW. Pheochromocytoma and multiple endocrine neoplasia. In: Feldman EC, Nelson RW (eds): Canine and feline endocrinology and reproduction, 3rd ed. St.Louis, MO: Saunders Elsevier, 2004; 440-463.

9. Blake MA, Cronin CG, Boland GW. Adrenal imaging. Am J Roentgenol 2010;194:1450-1460.

323 10. Johnson PT, Horton KM, Fishman EK. Adrenal mass imaging with multidetector CT:
324 pathologic conditions, pearls, and pitfalls. Radiographics 2009;29:1333-1351.

325 11. Caoili EM, Korobkin M, Francis IR, et al. Adrenal Masses: Characterization with
326 Combined Unenhanced and Delayed Enhanced CT. Radiology 2002;222:629-633.

327 12. Schteingart DE, Doherty GM, Gauger PG, et al. Management of patients with adrenal
328 cancer: recommendations of an international consensus conference. Endocr Relat Cancer
329 2005;12:667-680.

330 13. Bertolini G, Furlanello T, DeLorenzi D, et al. Computed tomographic quantification of
331 canine adrenal gland volume and attenuation. Vet Radiol Ultrasound 2006;47:444–448.

332 14. Voorhout G. X-ray-computed tomography, nephrotomography, and ultrasonography
333 of the adrenal glands of healthy dogs. Am J Vet Res 1990;51:625–631.

334 15. Bertolini, G, Furlanello T, Drigo M, et al. Computed tomographic adrenal gland
335 quantification in canine adrenocorticotroph hormone-dependent hyperadrenocorticism.
336 Vet Radiol Ultrasound 2008;49:449-453.

337 16. Wood FD, Pollard RE, Uerling MR, et al. Diagnostic imaging findings and endocrine
338 test results in dogs with pituitary-dependent hyperadrenocorticism that did or did not
339 have neurologic abnormalities: 157 cases (1989–2005). J Am Vet Med Assoc
340 2007;231:1081–1085.

341 17. Van Der Vlugt-Meijer RH, Voorhout G, Meij BP. Imaging of the pituitary gland in dogs
342 with pituitary-dependent hyperadrenocorticism. Mol Cell Endocrinol 2002;197:81–87.

343 18. Rosenstein DS. Diagnostic imaging in canine pheochromocytoma. Vet Radiol
344 Ultrasound 2000;41:499-506.

345 19. Schultz RM, Wisner ER, Johnson EG, et al. Contrast-enhanced computed tomography
346 as a preoperative indicator of vascular invasion from adrenal masses in dogs. Vet Radiol
347 Ultrasound 2009; 50:625-629.

348 20. Voorhout G, Stolp R, Rijnberk A, et al. Assessment of survey radiography and
349 comparison with x-ray computed tomography for detection of hyperfunctioning
350 adrenocortical tumors in dogs. J Am Vet Med Assoc 1990;196:1799–1803.

351 21. Besso JG, Penninck DG, Gliatto JM. Retrospective ultrasonographic evaluation of
352 adrenal lesions in 26 dogs. Vet Radiol Ultrasound 1997;38:448-455.

353 22. Kawashima A, Sandler CM, Fishman EK, et al. Spectrum of CT findings in nonmalignant
354 disease of the adrenal gland. Radiographics 1998;18:393-412.

355 23. Labelle P, Kyles AE, Farver TB, et al. Indicators of malignancy of canine adrenocortical
356 tumors: histopathology and proliferation index. Vet Pathol 2004;41:490-497.

357 24. Kyles AE, Feldman EC, Cock HE, et al. Surgical management of adrenal gland tumors
358 with and without associated tumor thrombi in dogs: 40 cases (1994-2001). J Am Vet Med
359 Assoc 2003;223:654-662.

360 25. Davis MK, Schochet RA, Wrigley R. Ultrasonographic identification of vascular
361 invasion by adrenal tumors in dogs. Vet Radiol Ultrasound 2012;53:442-445.

362 26. Mayo-Smith WW, Boland GW, Noto RB, et al. State-of-the-art adrenal imaging1.
363 Radiographics 2001;21:995-1012.

364 27. Giglio RF, Winter MD, Berry CR, et al. Comparison between the CT features of adrenal
365 adenocarcinoma and pheochromocytoma in dogs. *Proceeding of the ACVR Annual*
366 *Scientific Meeting*, Savannah, GA, October 8-11, 2013;38.

367 28. Korobkin M, Brodeur FJ, Yutzy GG, et al. Differentiation of adrenal adenomas from
368 nonadenomas using CT attenuation values. Am J Roentgenol 1996; 166:531-536.

369 29. Pey P, Rossi F, Vignoli M, et al. Assessment of contrast-enhanced ultrasonography and
370 contrast-enhanced computed tomography for the evaluation of adrenal tumors in dogs.
371 *Proceeding of the IVRA and EVDI Annual Meeting*, Bursa, Turkey, August 26-September 1,
372 2012;20.

373 30. Burton JH, Mitchell DH, Thamm SW, et al. Low-dose cyclophosphamide selectively decreases
374 regulatory T cells and inhibits angiogenesis in dogs with soft tissue sarcoma. J Vet Intern Med
375 2011;25:920-926.

Table 1. Relationships between tumor type and histopathological findings

	Adenoma	Adenocarcinoma	Pheochromocytoma	*P*-value
	n=3	n=9	n=5	
Mitotic index	MI0=2, MI2=1	MI0=3, MI1=1, MI2=4, MI4=1	MI0=2, MI1=2, MI3=1,	0.48
Cellular differentiation	Well differentiated=3	Well differentiated=4 Moderately differentiated=3 Poorly differentiated=2	Well differentiated=4 Moderately differentiated=1	0.38
% of necrosis	N0=3	N0=6; N1=1; N2=1; N3=1	N0=3; N1=2	0.81
Hemorrhage/infarction	No=2;Yes=1	No=7;Yes=2	No=2;Yes=3	0.54
Capsular invasion	No=3	No=6;Yes=3	No=4;Yes=1	0.66
Microscopic vascularity	Mild=2;Moderate=1	Mild=4;Moderate=2;Marked=3	Mild=1;Moderate=1;Marked=3	0.61
Microscopic vascular invasion	No=2;Yes=1	No=5;Yes=4	No=1;Yes=4	0.43
Macroscopic vascular invasion	No=3	No=8;Yes=1	No=1;Yes=4	0.02
Tumor grade	Low=3	Low=4;High=5	Low=1;High=4	0.1

Table 2. Relationships between tumor type and CT features

	Adenoma	Adenocarcinoma	Pheochromocytoma	*P*-value
	n=3	n=9	n=5	
Maximum diameter (mm)	Mean= 25.3 +/- 4.6 SD	Mean= 29.5 +/- 14.1 SD	Mean= 41.4 +/- 18.4 SD	0.26
Outline	Irregular demarcation=1 Well demarcated=2	Irregular demarcation =1 Well demarcated=8	Irregular demarcation =2 Well demarcated=3	0.77
Shape	Rounded=3	Rounded=8;Lobulated=1	Rounded=2;Lobulated=3	0.12
Pattern pre-contrast attenuation	Heterogeneous=2;Homogeneous=1	Heterogeneous=4;Homogeneous=5	Heterogeneous=4;Homogeneous=1	0.54
Pattern post-contrast enhancement (early)	Heterogeneous=3	Heterogeneous=3;Homogeneous=6	Heterogeneous=4;Homogeneous=1	0.14
Pattern post-contrast enhancement (late)	Heterogeneous=2;Homogeneous=1	Heterogeneous=1;Homogeneous=6	Heterogeneous=3;Homogeneous=1	0.22
Contrast-enhancing rim (early)	Yes=3	No=6;Yes=3	No=3;Yes=2	0.17
Contrast-enhancing rim (late)	Yes=3	No=5;Yes=2	No=3;Yes=1	0.12
Vascular invasion	No=2;Yes=1	No=8;Yes=1	No=1;Yes=4	0.03
Mean HU pre-contrast	Mean= 40.8 +/- 14.3 SD	Mean= 36.7 +/- 11.8 SD	Mean= 52.3 +/- 5 SD	0.06
Mean HU post-contrast (early)	Mean= 66.7+/- 8.3 SD	Mean= 83.9+/- 52.7 SD	Mean= 103 +/- 21.7 SD	0.49
Mean HU post-contrast (late)	Mean= 55.5 +/- 22.4 SD	Mean= 76.9 +/- 28.4 SD	Mean= 93.4 +/- 14.3 SD	0.16
Degree of contrast enhancement (early)	Mild=1;Moderate=2	Mild=5;Moderate=3; Marked=1	Moderate=4; Marked=1	0.227
Degree of contrast enhancement (late)	Moderate=3	Mild=4;Moderate=3	Moderate=3; Marked=1	0.09
HU difference pre-post (early)	Mean= 25.9 +/- 21.3 SD	Mean= 47.2 +/- 46.5 SD	Mean= 50.6 +/- 23.6 SD	0.65
HU difference pre-post (late)	Mean= 14.7 +/- 21.7 SD	Mean= 41.8+/-17.7 SD	Mean= 42.8 +/- 14.2 SD	0.09

Table 3. Agreement or correlation between analogous histopathological and CT features

Histopathological feature	CT feature	Statistic	*P*-value
Capsular invasion	Outline	0.3 [a]	0.5
Capsular invasion	Contrast-enhancing rim (early)	0.27 [a]	0.29
Capsular invasion	Contrast-enhancing rim (late)	0.53 [a]	0.05
Vascular invasion	Vascular invasion	0.86 [a]	0.001
% necrosis	Post-contrast enhancement (early)	0.069 [b]	0.77
% necrosis	Post-contrast enhancement (late)	-0.02 [b]	1
Hemorrhage or infarction	Pattern of post-contrast enhancement (early)	0.37 [a]	0.3
Hemorrhage or infarction	Pattern of post-contrast enhancement (late)	0.45 [a]	0.05
Microscopic vascularity	Degree of contrast enhancement (early)	-0.03 [b]	0.91
Microscopic vascularity	Degree of contrast enhancement (late)	-0.36 [b]	0.18

[a] Kappa; [b] Kendall's tau

Legends:

A 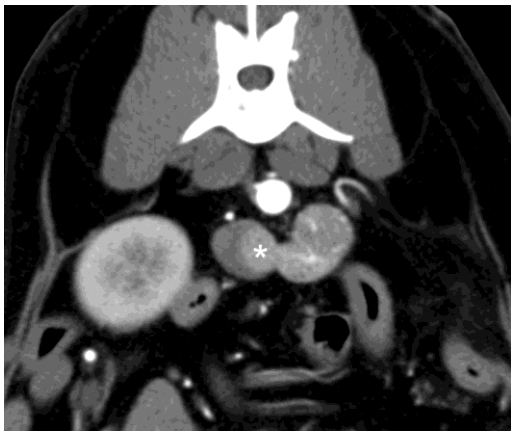 B 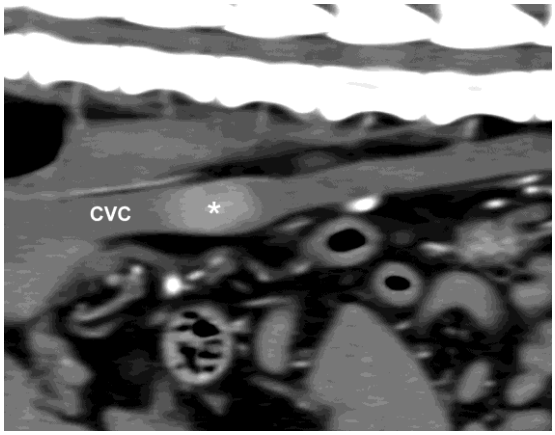

Fig. 1. A) Transverse and B) sagittal post-contrast CT images showing vascular invasion of a left adrenal mass. There is a contrast enhancing mass (*) within the lumen of the caudal vena cava (CVC).

A 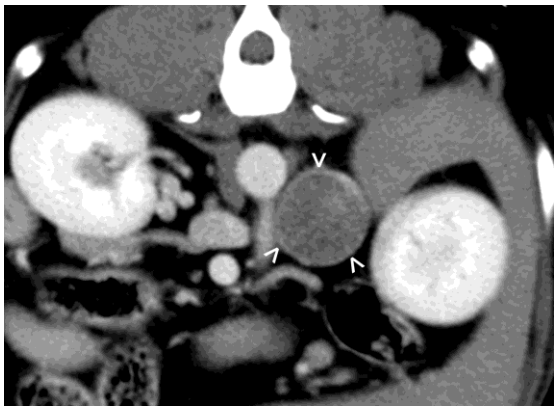 B 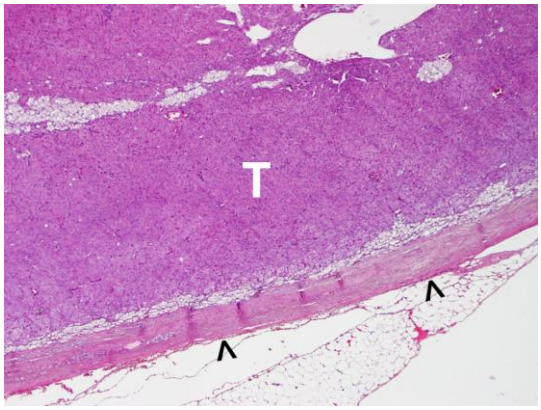

Fig. 2. A) Transverse post-contrast CT image showing thin, peripheral rim of enhancement (arrowheads) in a left adrenal mass. B) Corresponding histologic section showing a layer of fibrous tissue (arrowheads) forming a pseudo-capsule around the tumor (T).

A

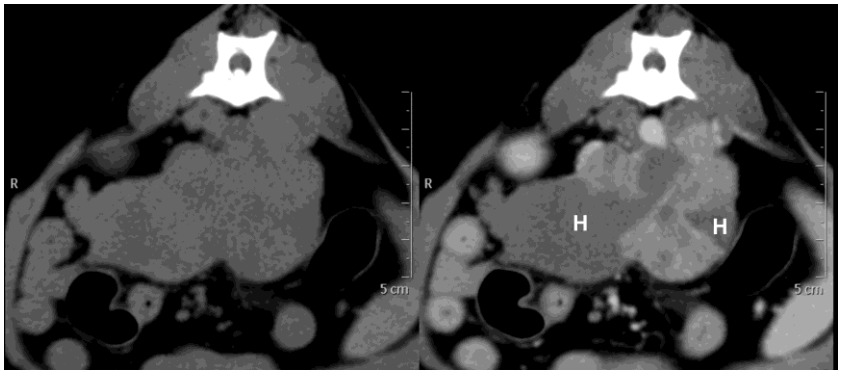

B

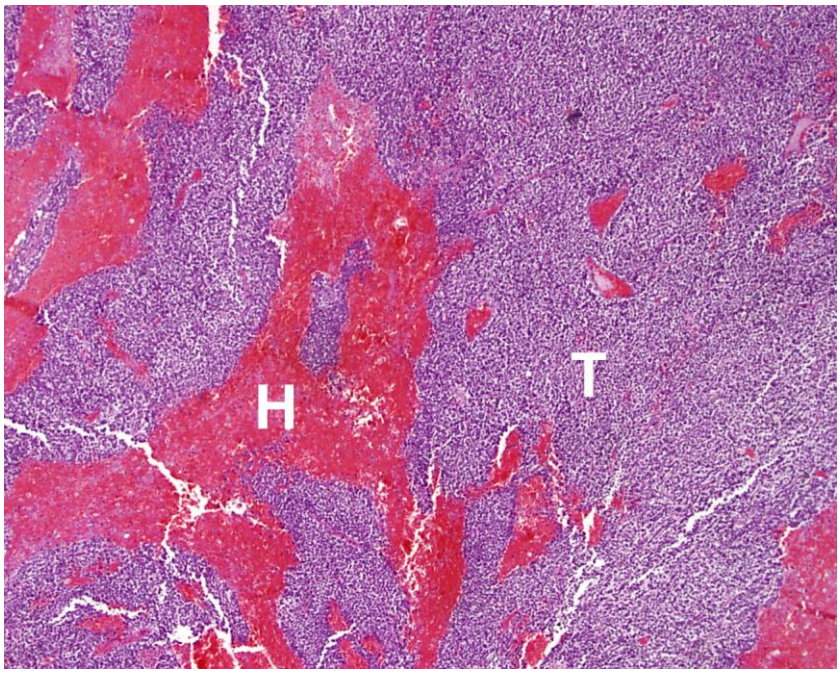

Fig. 3. A) Transverse pre- (left) and post-contrast (right) CT images of a large left adrenal mass. The lesion has faintly heterogeneous attenuation in the pre-contrast image. Several non-contrast enhancing areas representing hemorrhage (H) within the tumor become apparent after contrast administration. B) Corresponding histologic section of the same mass showing irregular areas of hemorrhage (H) within the tumor (T).